Journal of Information Systems Engineering and Management
2025, 10(29s)
e-ISSN: 2468-4376
https://www.jisem-journal.com/

Research Article

Central Tropical Indian Ocean heat Budget Analysis During Indian Ocean Tripole events

Prerna Malik [1], Bhasha H. Vachharajani [2*]
[1] *Department of Mathematics, School of Technology, PDEU, Raysan, Gujarat-382426, India. Email: malikprerna1@gmail.com*
[2] *Department of Mathematics, School of Technology, PDEU, Raysan, Gujarat-382426, India. Email: Bhasha.Vachharajani@sot.pdpu.ac.in*

ARTICLE INFO

Received: 31 Dec 2024

Revised: 20 Feb 2025

Accepted: 28 Feb 2025

ABSTRACT

The Indian Ocean Tripole (IOT) mode, associated with the third mode of sea surface temperature anomaly (SSTA) variability, exhibits a unique pattern characterized by positive SSTA dominating the central Tropical Indian Ocean (TIO), while negative SSTA prevail in the western and eastern regions. This distinct mode of variability significantly influences the surrounding climate. In this study, the underlying causes of SSTA variability in the central TIO during tripole events are investigated through an SST heat budget analysis. Specifically, the anomalous warming in the central TIO is examined. A multiple linear regression analysis is performed using climate indices linked to most dominant SSTA-based climate modes, El Nino Southern Oscillations (ENSO), Indian Ocean Dipole (IOD), and IOT on SST budget terms to determine key drivers. The results reveal that net heat flux is the primary contributor to the positive SSTA in the central TIO. To further disentangle this influence, the individual contributions of radiative and turbulent heat flux components are analysed. This study enhances our understanding of TIO dynamics during IOT events and their broader implications for regional and global climate systems.

Keywords: Tropical Indian Ocean, Indian Ocean Tripole, Sea Surface Temperature, Heat budget analysis, Multiple Linear Regression.

INTRODUCTION

TIO is a major contributor to overall increase in the global SST trend. It is a significant component of greatest warm pool on the planet. Its interconnection with atmosphere has a notable impact on regional and global climate. Numerous investigations found that during past century, surface temperature of the Indian Ocean has been rising more rapidly than other tropical oceans [1, 2]. The rapid warming of the Indian Ocean has been associated with various consequences, such as diminished cloud cover, a weakened Indian monsoon, alterations in ocean currents, and shifts in heat distribution [3, 4, 5]. SSTA based climate modes largely impact TIO variability. The IOD mode contributes significantly to the TIOs interannual variability, it was by a group of researchers reported in the late 1990s [6]. Positive and negative phases of IOD are closely associated with rainfall variability of regions surrounding Indian Ocean. A positive Indian Ocean Dipole (IOD) is characterized by strong easterly and southerly wind anomalies, typically leading to reduced rainfall over parts of Australia and Indonesia, while Africa experiences above-average rainfall [7, 8, 9]. In contrast, these patterns reverse during a negative IOD phase.

ENSO is a periodic climatic phenomenon that involves varying SSTs in the equatorial Pacific that has been linked with IOD events in TIO. The connection between IOD and ENSO is complicated, and ENSO may occasionally generate IOD episodes, with IOD strength governed by coupled instability and external factors such as intraseasonal oscillations within the TIO region. In other cases, IOD may occur independently from within the Indian Ocean [10, 11, 12]. The diverse manifestations of ENSO have drawn significant attention from researchers due to their broad atmospheric teleconnections and impacts on local sea level variations. However, compared to the tropical Pacific, studies on the variability of climate drivers like the IOD in the Tropical Indian Ocean remain relatively scarce. However, some researchers investigated differences in the development of IOD events based on their emergence and maturation [13, 14, 15]. Endo & Tozuka [16] defined IOD events based on their spatial pattern of SSTA. IOD events were once thought to represent a single phenomenon, but later research revealed the existence of two distinct types:

the canonical IOD and IOD Modoki [17, 18]. While the canonical IOD involves opposite SSTA between the western and eastern parts of the TIO, IOD Modoki displays a more complex tripole-like pattern of SST anomalies. SSTA in the western and eastern regions of TIO are of the same sign (either both positive or both negative), with opposite anomalies in the central TIO.

The research by Zhang et al [19] offered fresh perspectives on the dynamics of the TIO. Utilizing an extensive dataset, the study identified a third mode of variability in the region, known as the Indian Ocean Tripole (IOT) mode, which explains 8% of the total SSTA variability. The periodic development of IOT and IOD occurrences greatly differs. While IOD matures from September to November, the IOT events often peak from June to August. Apart from IOD, this study also attempts to addresses the IOT's interaction with other climatic modes such as ENSO. The study revealed that the IOT is positively connected with El Nino and negatively correlated with La Nina events. The IOT may influence the climate of surrounding regions, making it crucial to explore the factors driving SSTA variability during IOT events. This can be accomplished through an SST heat budget analysis [20]. The interconnected nature of climate modes makes it challenging to isolate the individual impact of the IOT mode. To address this, we employed a Multiple Linear Regression (MLR) approach [21]. The structure of the paper is as follows: Section 2 describes the datasets utilized and details the methodology applied for the analysis. Section 3 highlights the results and discussions, emphasizing the spatio-temporal variability linked to positive IOT events and the findings from regression analysis. Section 4 concludes with a summary of the key findings and their implications.

METHODOLOGY

Datasets

In this study, we have used SST, winds (10 m height), Surface Latent Heat Flux (SLHF), Surface Sensible Heat Flux (SSHF), Surface Net Solar Radiation (SSR), and Surface Net Thermal Radiation (STR) datasets from the fifth-generation European Centre for Medium-Range Weather Forecasts Reanalysis (ERA5) [22]. These parameters are available on a monthly domain at a spatial resolution of 0.25°×0.25°. The zonal and meridional components of surface current and mixed-layer depth monthly data is obtained from Ocean Reanalysis System 5 (ORAS5) available at 0.25°×0.25° resolution [23].

Methodology

Monthly climate indices associated with SSTA based climate modes are utilized for this study. Dipole Mode Index (DMI) used to identify IOD events is calculated using method proposed by Saji et al. [6] and Nino3.4 index is utilized for distinguishing ENSO related variability. The Tripole Mode Index (TMI) associated with IOT events was suggested by Zhang et al. [19] The TMI index is determined by difference in averaged SSTA of central (65°-85°E,20°S-5°N) from western (45°-60°E,5°S-20°N and 60°-70°E,10°-20°N) and eastern (90°-110°E,10°S-equator) regions of TIO.

To extract the signals exclusively related to TMI index, we use a MLR approach, where climate indices are set as independent variables and their impact is observed on other ocean-atmospheric variables. MLR is applied on SST heat budget equation as shown in equation 1 [24]:

$$\frac{\partial(\mathrm{T})}{\partial \mathrm{t}} = \frac{\mathrm{Q_{net}}}{\rho\, \mathrm{C_p}\, \mathrm{H}} - \left[\mathrm{u}\frac{\partial(\mathrm{T})}{\partial \mathrm{x}} + \mathrm{v}\frac{\partial(\mathrm{T})}{\partial y}\right] + \mathrm{R} \quad (1)$$

Where Q_{net} is the net heat flux represented by the following equation 2:

$$\mathrm{Q_{net}} = \mathrm{SLHF} + \mathrm{SSHF} + \mathrm{SSR} + \mathrm{STR} \quad (2)$$

Regression coefficient associated with TMI index shows its individual impact on SST budget terms. The air density, ρ, is 1.225 kg m^{-3}, while C_p refers to the specific heat capacity of seawater. H denotes the depth of the ocean's mixed layer, and u and v represent the zonal and meridional components of ocean surface currents, respectively. The residual term, R, accounts for the effects of other oceanic processes, such as upwelling and vertical mixing.

RESULTS AND DISCUSSIONS

Spatio Temporal analysis of Indian Ocean Tripole mode

Figure 1 represents the composite map of all the positive Indian Ocean Tripole mode events spanning from 1993 to 2022 for June-August (JJA) season. The W, C, and E boxes represent the western, central, and eastern regions of TIO utilized in calculating the time series Tripole mode Index (TMI). TMI series shown in Figure 2 associated with IOT events identifies six positives: 1994, 2003, 2008, 2013, 2015, and 2018 and five negative: 1993, 1995, 1998, 2009, and 2021 IOT events. Since positive IOT events are a mirror image of negative, they remain focus of this study.

Figure 3a depicts the regression coefficient of TMI on SSTA and wind components for JJA season. Colour bar is showing regions with statistical significance above 90% confidence level. The spatial pattern resembles positive IOT like pattern. Stronger positive SSTA are found in central region, whereas, negative SSTA are found in western and eastern regions, with more significance in western region. The unique wind pattern obtained of MLR analysis shows that in western region, winds follow climatological pattern over Arabian Sea, strengthening the south-west monsoon winds towards the Indian subcontinent. The easterlies originating from eastern TIO, are splitting into two branches, one deflecting towards the Bay of Bengal, and another converging in central TIO. The south-central TIO is found to be the region of convergence, for both westerly and easterly winds. MLR patterns depicts significant positive SSTA, along with converging winds in the central region of TIO, highlighting the importance of further investigating the SSTA variability caused in this region due to IOT events.

Figure 3b shows temporal plots of SST, rate of change of SST, and wind speed anomalies for positive IOT events, averaged over central TIO region. It is observed that SSTA remained closed to zero in April and May, indicating no major changes in solar heating. From June the SSTA remains positive till December above 0.25 K, suggesting more than usual SSTA warming during those months. The wind patterns align with SSTA patterns. As SSTA is positive from, June, anomalous wind speed reduces significantly in June and remains negative from June to September. The lower wind speed anomalies can also be lined with the region of convergence of winds observed in Figure 3a. The anomalous rate of change of SST is found to be positive from May to July, and reaches near zero in August, indicating slower than usual rate of change during positive IOT events, which explains the positive SSTA over the region. The rate of change of SST can have major impact on climate of surrounding region, hence it needs to be investigated further.

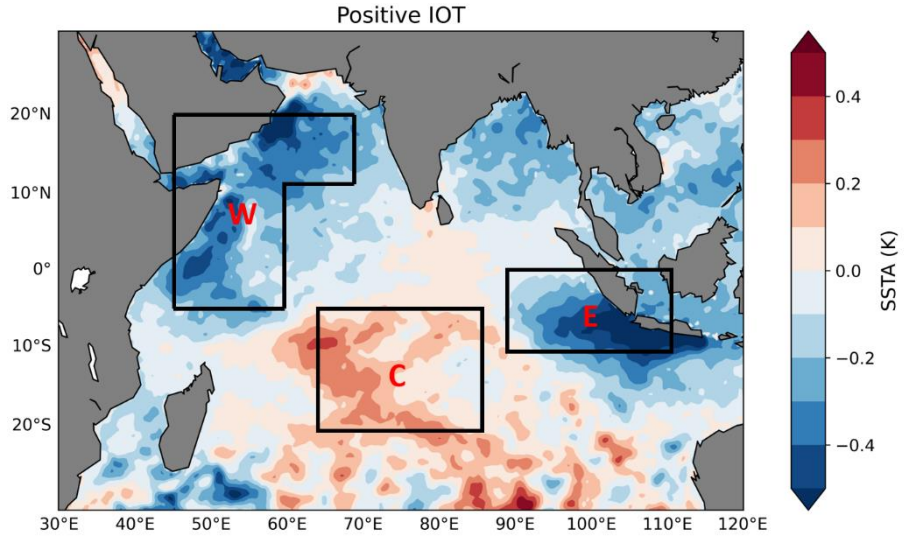

Figure 1. Composite of positive IOT events from 1993 to 2022. W, C, and E boxes represent western, central, and eastern regions of Tropical Indian Ocean respectively.

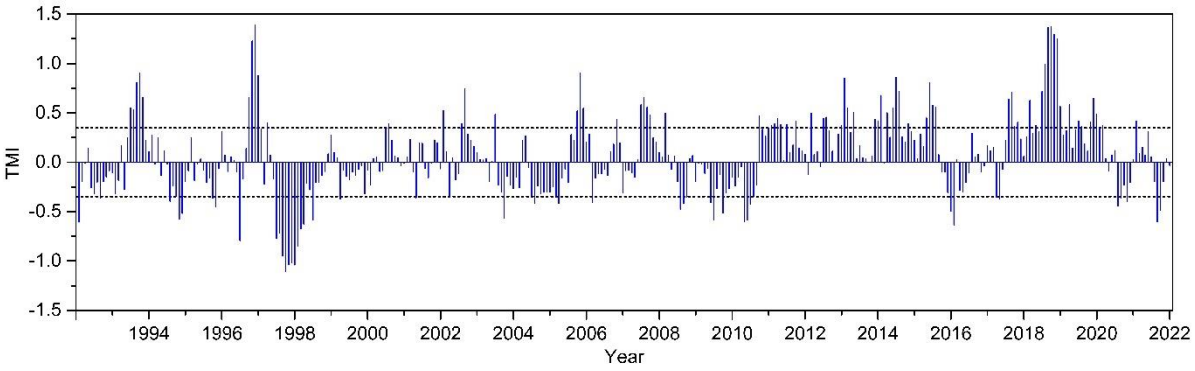

Figure 2. Monthly TMI time series from 1993 to 2022.

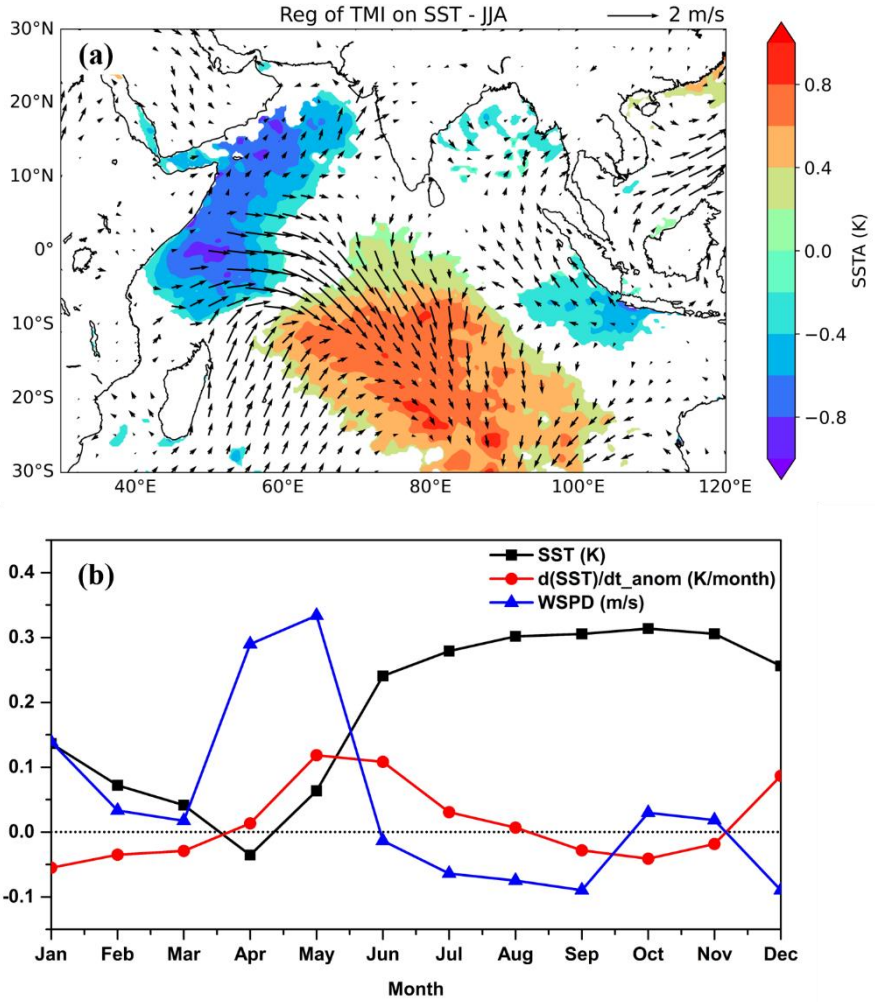

Figure 3. (a) regression of TMI series on SSTA (colour) on significant regions at 90% confidence and wind components (vectors) for JJA season. (b) monthly composite anomalies of SST (black), d(SST)/dt (red), and wind speed (blue) for positive IOT years over the central tropical Indian Ocean.

SST budget terms analysis

This section discusses the SST budget terms analysis. Figure 4 depicts the results MLR of TMI on SST budget, which includes net heat flux and horizontal advection terms. Vertical processes and mixing are excluded for the purpose of simplifying the analysis, as it aligns with a focus on large-scale SST variability. Figure 4a and Figure 4b shows regression coefficient of TMI on rate of change of SST and net heat flux term respectively for JJA season. Figure 4c depicts monthly regression coefficients of TMI for budget terms. From Figure 4c, it is observed that, rate of change of SST is maximum in May and reduces rapidly in June. This sudden decrease is linked with the onset of summer

monsoon. Monsoon winds cover the region, reducing SSTA in June and July. Once the monsoon is established, the SSTA starts to rise slowly from August. It is observed that pattern of rapidly decreasing SSTA aligns with NHF in JJA season. Whereas, the advection term does not show any significant changes and remains close to zero. This pattern can also be seen spatially in Figure 4a and Figure 4b. The rate of change of SST is significantly negative in the central region, aligning with slightly negative pattern of net heat flux term. The net heat flux term does not show strong signal like rate of change of SST because after showing negative pattern in June, it also recovers in July and remains close to zero. The analysis suggests net heat flux term to be dominant factor in influencing the rate of change of SST over the central region of TIO.

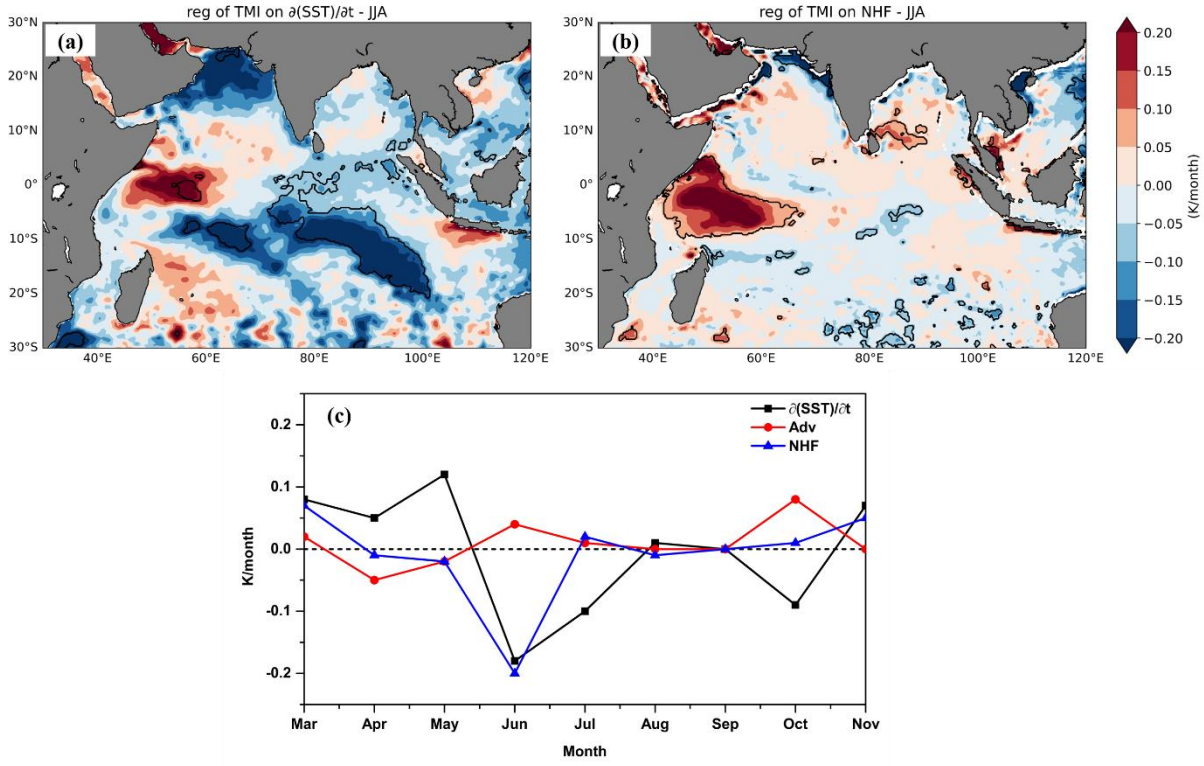

Figure 4. Regression of TMI on (a) rate of change of SST and (b) net heat flux term. (c) regression coefficient of TMI on budget terms averaged over central Tropical Indian Ocean.

The MLR analysis shows the pattern of budget terms over the region, however, it needs further investigation on how these terms differ during IOT years from climatological pattern. Figure 5 shows the results of composite analysis of anomalous net heat flux and advection term for positive IOT events averaged over central region. It is found that net heat flux term remains negative from Jan to April, and it becomes positive from May to August. The positive values align with anomalous values of rate of change of SST in Figure 3b, suggesting positive contribution of net heat flux term in influencing SST change. However, the advection term is found to be negative from May to August. The analysis suggest that positive anomalies of rate of change of SST are closely linked with net heat flux term, which is also consistent with the results of MLR analysis shown in Figure 4c. Therefore, net heat flux term needs to be investigated further to comprehend individual impacts of each radiative and turbulent flux components.

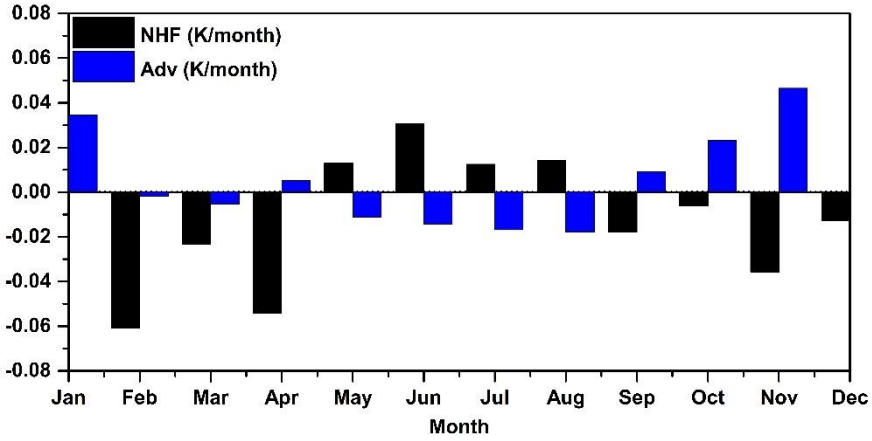

Figure 5. Composite anomalies of net heat flux (black) and advection (blue) terms for positive IOT events averaged over central Tropical Indian Ocean.

Net heat flux analysis

In this section turbulent heat fluxes: SLHF and SSHF, and radiative heat fluxes: SSR and STR are analysed for positive IOT years. Surface heat flux components are crucial for managing the ocean-atmosphere system. SLHF directs heat loss by evaporation, which directly influences SST, especially during monsoon season. SSHF refers to heat exchange caused by temperature gradients, although its role in relatively small. SSR, net solar heating absorbed by ocean, is primary source of ocean heating. STR represents net longwave radiation radiation at the surface, contributing to heat retention and regulating surface cooling. Together these fluxes interact to modulate SST variability.

Figure 6 shows the composite of anomalous fluxes averaged over central TIO for positive IOT years. SLHF shows positive anomalies from January to April, reduces in May, and remains negative from May to August. Negative SLHF anomalies in monsoon season can reduce heat loss through evaporation. The SSHF anomalies remains close to zero, however in August, they seem to be negative. This can be due to reduced temperature gradient. As the monsoon season arrives, air temperature reduces whereas SSTs are warmer, leading to positive temperature gradient. As the SST starts to become cooler by August, the temperature gradient between ocean and atmosphere reduces leading to negative SSHF values. Negative SSHF anomalies in August are showing reduction in heat transfer from ocean surface to atmosphere, which can contribute to warmer SSTs. SSR anomalies remain negative throughout the year except for May and June, indicates that ocean surface receives more solar radiation during these months than the long-term average. This can be attributed to Clearer skies and reduced cloud cover before the full onset of the monsoon. The anomalous STR values are found to be positive from April to June and slightly negative from July onwards. Positive anomalies associated with pre monsoon period are due to increased warming of ocean surface, emitting more thermal radiation to the atmosphere. By July and August, southwest monsoon in full swing brings increased cloud cover and precipitation, acting as a barrier to thermal radiation. the composite heat flux anomalies during positive IOT years highlight the complex interplay between radiative and turbulent fluxes, with SSRD and SLHF playing dominant roles in shaping SST anomalies and ocean-atmosphere interactions in the central tropical Indian Ocean.

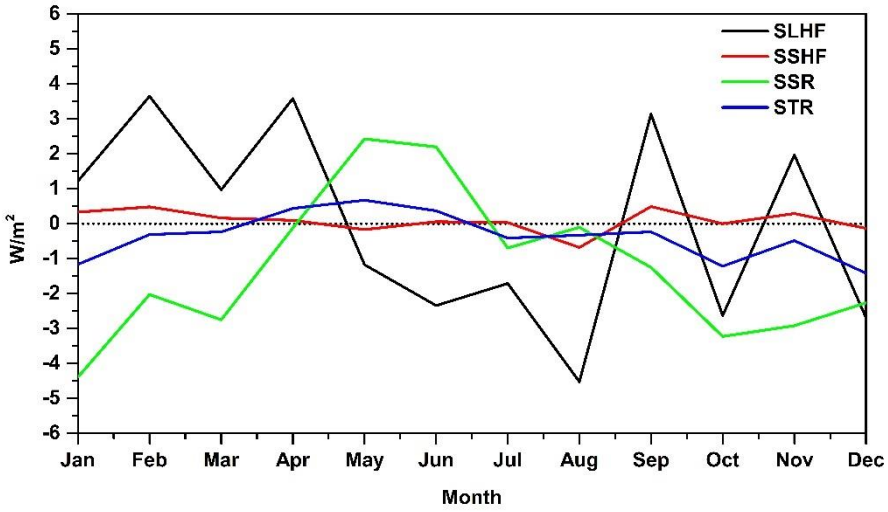

Figure 6. Composite of anomalies of heat flux components averaged over central tropical Indian Ocean for positive IOT years.

CONCLUSIONS

This study investigates at the spatio-temporal characteristics and underlying mechanisms that influence sea surface temperature anomalies (SSTA) during positive Indian Ocean Tripole (IOT) events, with a focus on the June-August (JJA) season. The analysis shows that the central tropical Indian Ocean (TIO) experiences large positive SSTA during these events, which is caused by complex interactions between atmospheric circulation patterns and oceanic heat fluxes. The regression and budget term studies emphasise the significant role of net heat flux (NHF), which exhibits positive anomalies throughout the monsoon season and contributes to SST warming. The lowered wind speed anomalies and converging wind patterns in the central TIO intensify the warming. Surface heat flux components, specifically surface latent heat flux (SLHF) and surface net solar radiation (SSR), play an important role in modifying SST variability. The combined effect of negative SLHF anomalies and negative SSR anomalies signifies that, while the ocean receives less solar radiation during the monsoon season (due to cloud cover), the decrease in evaporative heat loss (negative SLHF) allows the ocean to retain more of the heat absorbed earlier in the year. The pre-monsoon period experiences increased solar heating, whereas the monsoon season reduces heat loss, resulting in sustained warming of the ocean surface. This understanding is crucial for improving climate models and predictions for the region, particularly in the context of Indian Ocean variability and its impacts on surrounding climate systems. The interaction between radiative and turbulent heat fluxes shapes the SST anomalies, emphasizing the need for further investigation into the individual contributions of each flux component to the observed warming patterns during IOT events.

Acknowledgement

The authors are thankful to fifth-generation European Centre for Medium-Range Weather Forecasts Reanalysis (ERA5) as well as National Oceanic and Atmospheric Administration (NOAA) for making their datasets freely available.

Funding Statement

The authors received no financial assistance for this research.

Data Availability

Fifth-generation European Centre for Medium-Range Weather Forecasts Reanalysis (ERA5) https://cds.climate.copernicus.eu/datasets/reanalysis-era5-single-levels-monthly-means?tab=download Ocean Reanalysis System 5 (ORAS5) https://cds.climate.copernicus.eu/datasets/reanalysis-oras5?tab=download

Conflict of Interest

The authors declare no conflicts of interest.

REFERENCES

[1] M. K. Roxy, R. K. Ritika, P. Terray, and S. Masson, "The curious case of Indian Ocean warming," Journal of Climate, vol. 27, no. 22, pp. 8501-8509, 2014, doi: 10.1175/JCLI-D-14-00471.1.

[2] M. K. Roxy, C. Gnanaseelan, A. Parekh, J. S. Chowdary, S. Singh, A. Modi, R. Kakatkar, S. Mohapatra, C. Dhara, S. C. Shenoi, and M. Rajeevan, "Indian Ocean warming," in Assessment of Climate Change over the Indian Region, pp. 191-206, Springer Singapore, 2020, doi: 10.1007/978-981-15-4327-2_10.

[3] M. K. Roxy, R. K. Ritika, P. Terray, R. Murtugudde, K. Ashok, and B. N. Goswami, "Drying of Indian subcontinent by rapid Indian Ocean warming and a weakening land-sea thermal gradient," Nature Communications, vol. 6, no. 1, pp. 7423, 2015, doi: 10.1038/ncomms8423.

[4] R. K. Yadav and M. K. Roxy, "On the relationship between north India summer monsoon rainfall and east equatorial Indian Ocean warming," Global and Planetary Change, vol. 179, pp. 23-32, 2019, doi: 10.1016/j.gloplacha.2019.05.001.

[5] L. Yang, R. Murtugudde, L. Zhou, and P. Liang, "A potential link between the Southern Ocean warming and the South Indian Ocean heat balance," Journal of Geophysical Research: Oceans, vol. 125, no. 12, 2020, doi: 10.1029/2020JC016132.

[6] N. H. Saji, B. N. Goswami, P. N. Vinayachandran, and T. Yamagata, "A dipole mode in the tropical Indian Ocean," Nature, vol. 401, no. 6751, pp. 360-363, 1999, doi: 10.1038/43854.

[7] C. C. Ummenhofer, A. Sen Gupta, M. H. England, and C. J. C. Reason, "Contributions of Indian Ocean sea surface temperatures to enhanced East African rainfall," Journal of Climate, vol. 22, no. 4, pp. 993-1013, 2009, doi: 10.1175/2008JCLI2493.1.

[8] K. Chansaengkrachang, A. Luadsong, and N. Aschariyaphotha, "A study of the time lags of the Indian Ocean Dipole and rainfall over Thailand by using the cross wavelet analysis," Arabian Journal for Science and Engineering, vol. 40, no. 1, pp. 215-225, 2015, doi: 10.1007/s13369-014-1480-1.

[9] I. G. Hendrawan, K. Asai, A. Triwahyuni, and D. V. Lestari, "The interannual rainfall variability in Indonesia corresponding to El Niño Southern Oscillation and Indian Ocean Dipole," Acta Oceanologica Sinica, vol. 38, no. 7, pp. 57-66, 2019, doi: 10.1007/s13131-019-1457-1.

[10] S. K. Behera, J. J. Luo, S. Masson, S. A. Rao, H. Sakuma, and T. Yamagata, "A CGCM study on the interaction between IOD and ENSO," Journal of Climate, vol. 19, no. 9, pp. 1688-1705, 2006, doi: 10.1175/JCLI3797.1.

[11] G. Meyers, P. McIntosh, L. Pigot, and M. Pook, "The years of El Niño, La Niña, and interactions with the tropical Indian Ocean," Journal of Climate, vol. 20, no. 13, pp. 2872-2880, 2007, doi: 10.1175/JCLI4152.1.

[12] C. C. Hong, M. M. Lu, and M. Kanamitsu, "Temporal and spatial characteristics of positive and negative Indian Ocean dipole with and without ENSO," Journal of Geophysical Research: Atmospheres, vol. 113, no. 8, 2008, doi: 10.1029/2007JD009151.

[13] P. N. Vinayachandran, N. H. Saji, and T. Yamagata, "Response of the equatorial Indian Ocean to an unusual wind event during 1994," Geophysical Research Letters, vol. 26, no. 11, pp. 1613-1616, 1999, doi: 10.1029/1999GL900179.

[14] S. A. Rao, "Abrupt termination of Indian Ocean dipole events in response to intraseasonal disturbances," Geophysical Research Letters, vol. 31, no. 19, L19306, 2004, doi: 10.1029/2004GL020842.

[15] Y. Du, W. Cai, and Y. Wu, "A new type of the Indian Ocean Dipole since the mid-1970s," Journal of Climate, vol. 26, no. 3, pp. 959-972, 2013, doi: 10.1175/JCLI-D-12-00047.1.

[16] S. Endo and T. Tozuka, "Two flavors of the Indian Ocean Dipole," Climate Dynamics, vol. 46, no. 11–12, pp. 3371-3385, 2016, doi: 10.1007/s00382-015-2773-0.

[17] N. Anil, M. R. Ramesh Kumar, R. Sajeev, and P. K. Saji, "Role of distinct flavours of IOD events on Indian summer monsoon," Natural Hazards, vol. 82, no. 2, pp. 1317-1326, 2016, doi: 10.1007/s11069-016-2245-9.

[18] T. Tozuka, S. Endo, and T. Yamagata, "Anomalous Walker circulations associated with two flavors of the Indian Ocean Dipole," Geophysical Research Letters, vol. 43, no. 10, pp. 5378-5384, 2016, doi: 10.1002/2016GL068639.

[19] Y. Zhang, J. Li, S. Zhao, F. Zheng, J. Feng, Y. Li, and Y. Xu, "Indian Ocean tripole mode and its associated atmospheric and oceanic processes," Climate Dynamics, vol. 55, no. 5-6, pp. 1367-1383, 2020, doi: 10.1007/s00382-020-05331-1.

[20] H. Xia and K. Wu, "Investigation of the heat budget of the tropical Indian Ocean during Indian Ocean dipole events occurring after ENSO," Journal of Ocean University of China, vol. 19, no. 3, pp. 525-535, 2020, doi: 10.1007/s11802-020-4269-8.

[21] Y. Zhang, W. Zhou, X. Wang, X. Wang, R. Zhang, Y. Li, and J. Gan, "IOD, ENSO, and seasonal precipitation variation over eastern China," Atmospheric Research, vol. 270, 106042, 2022, doi: 10.1016/j.atmosres.2022.106042.

[22] H. Hersbach, B. Bell, P. Berrisford, G. Biavati, A. Horányi, J. Muñoz Sabater, J. Nicolas, C. Peubey, R. Radu, I. Rozum, D. Schepers, A. Simmons, C. Soci, D. Dee, J.-N. Thépaut, "ERA5 monthly averaged data on single levels from 1940 to present," Copernicus Climate Change Service (C3S) Climate Data Store (CDS), 2023, doi: 10.24381/cds.f17050d7.

[23] H. Zuo, M. Balmaseda, S. Tietsche, K. Mogensen, and M. Mayer, "The ECMWF operational ensemble reanalysis-analysis system for ocean and sea-ice: A description of the system and assessment," Ocean Sci. Discuss., 2019, doi: 10.5194/os-2018-154.

[24] A. Cherchi and A. Navarra, "Influence of ENSO and of the Indian Ocean dipole on the Indian summer monsoon variability," Climate Dynamics, vol. 41, no. 1, pp. 81-103, 2012, doi: 10.1007/s00382-012-1602-y.